Biochimica et Biophysica Acta 1820 (2012) 33–43

Contents lists available at SciVerse ScienceDirect

Biochimica et Biophysica Acta

journal homepage: www.elsevier.com/locate/bbagen

Liver X receptor agonist T0901317 induced liver perturbation in zebrafish: Histological, gene set enrichment and expression analyses

Hendrian Sukardi [a], Xiaoyan Zhang [a], Eei Yin Lui [a], Choong Yong Ung [a], Sinnakaruppan Mathavan [c], Zhiyuan Gong [a,b,*], Siew Hong Lam [a,b,**]

[a] Department of Biological Sciences, 14 Science Drive 4, National University of Singapore, 117543 Singapore
[b] NUS Environmental Research Institute (NERI), TL #02-02, Engineering Drive 1, 117411 Singapore
[c] Genome Institute of Singapore, Agency for Science Technology and Research, Genome, 60 Biopolis Street, 138672 Singapore

ARTICLE INFO

Article history:
Received 3 June 2011
Received in revised form 4 October 2011
Accepted 16 October 2011
Available online 25 October 2011

Keywords:
Zebrafish
Liver X receptor
T0901317
Liver
Toxicogenomics
Transcriptome

ABSTRACT

Background: Liver X receptor (LXR), a ligand-activated transcription factor, regulates important biological processes. It has been associated with pathology and proposed as a therapeutic target. The zebrafish is a new vertebrate model for disease modeling, drug and toxicity screening and will be interesting to test for its potential for LXR-related studies.
Methods: Adult male fish were exposed to LXR agonist T0901317 at 20, 200 and 2000 nM for 96 h and the livers were sampled for histological, microarray and qRT-PCR analyses.
Results: Histological analysis suggests dose-dependent perturbation of carbohydrate and lipid metabolisms by T0901317 in the liver, which lead to hepatocyte swelling and cell death. Microarray data revealed several conserved effects of T0901317 with mammalian models, including up-regulation of LXR-targeted genes, modulation of biological pathways associated with proteasome, cell death, extracellular matrix and adhesions, maturity onset diabetes of the young and lipid beta oxidation. Interestingly, this study identified the complement and coagulation systems as down-regulated by T0901317 for the first time, potentially via transcriptional repression by LXR activation. qRT-PCR validated the expression of 16 representative genes, confirming activation of LXR signaling and down-regulation of these biological pathways by T0901317 which could be linked to the anti-thrombogenic, anti-atherogenic and anti-inflammatory actions, as well as metabolic disruptions via LXR activation.
Conclusion and general significance: Our study underscores the potential of using zebrafish model coupled with transcriptomic analysis to capture pharmacological and toxicological or pathological events induced by LXR modulators.

1. Introduction

Liver X receptors (LXRs) are oxysterol-activated transcription factors. Its ligands include natural oxysterols 22-R-hydroxycholesterol (22R-HC), 24, 25(S)-epoxycholesterol, and 27-hydroxycholesterol, and synthetic compounds T0901317 and GW3965 [1,2]. Activated LXRs form heterodimers with retinoid X receptor and regulate gene transcription via binding to LXR response elements in the promoter regions of target genes [3]. In mammals, there are two LXR isoforms, LXRα (NR1H3) and LXRβ (NR1H2) but in zebrafish and fugu only one single LXR gene with higher sequence similarity to mammalian LXRα had been reported [4,5]. Zebrafish LXR has been found to be ubiquitously expressed in all examined tissues, with highest expression in the liver, and it can be activated by 22R-HC, and synthetic agonists such as GW3965 and T0901317 based on up-regulation of several known LXR regulated genes [4].

LXR regulates glucose and lipid metabolisms [6], and also modulates immune and inflammatory responses [7–9]. LXR is therefore a potential therapeutic target for atherosclerosis, diabetes and rheumatoid arthritis [8,10–13]. However, LXR activation is also associated with adverse effects such as hepatic steatosis and hypertriglyceridemia in mice [7]. Furthermore, administration of T0901317 induced more severe hepatic lipogenesis in diabetic mouse models than the non-diabetics [14]. The lipogenic effects of T0901317 lead to an increase of triglyceride and non-high density lipoprotein cholesterol in hamsters and monkeys in preclinical studies and thus outweigh the desired beneficial effects and prevent the advancement of T0901317 into clinical trials [12].

Zebrafish is an emerging new vertebrate model for comparative studies of energy metabolism [15], immune function [16]

* Correspondence to: Department of Biological Sciences, S3-Level 5, 14 Science Drive 4, National University of Singapore, 117543 Singapore. Tel.: +65 65162860; fax: +65 67792486.
** Correspondence to: Department of Biological Sciences, S3-Level 5, 14 Science Drive 4, National University of Singapore, 117543 Singapore. Tel.: +65 65167379; fax: +65 67792486.
E-mail addresses: dbsgzy@nus.edu.sg (Z. Gong), dbslsh@nus.edu.sg (S.H. Lam).

0304-4165/$ – see front matter © 2011 Elsevier B.V. All rights reserved.
doi:10.1016/j.bbagen.2011.10.009

and thrombosis [17] as it shares many important similarities in these physiological systems with mammals. Moreover, there is an increasing interest in using zebrafish for disease modeling, drug and toxicity screening [18,19] as it could provide an alternative model to rodent for studying drug-induced toxicity and drug screening. The liver is a major organ for drug metabolism and detoxification; hence perturbations can be detected from the liver and toxicity implicated with the perturbation can also be assessed. We have previously shown that chemical agonists that activate two other nuclear receptors (aryl hydrocarbon receptor and estrogen receptor) induced conserved responses between zebrafish and humans [20]. As for LXR, although its tissue distribution and developmental expression patterns had been characterized in zebrafish [4], little is known with regard to LXR-induced liver perturbation in zebrafish. In our efforts to understand nuclear receptor-induced perturbation and toxicity in the liver for disease modeling and drug screening using the zebrafish model, we have performed three independent experiments for histological, microarray and real-time PCR analyses in order to investigate T0901317-induced perturbation in the zebrafish liver. Here we present histological, biochemical and molecular evidence of conserved effects of LXR agonist between zebrafish and mammalian models, thus supporting the zebrafish model for LXR-related studies. Gene set enrichment analysis provided additional insights into T0901317 concentration-dependent induced liver perturbation which resulted in modulation of several molecular signatures including coagulation and complement systems which has not been reported previously. By validating the genes using quantitative real-time PCR in another independent experiment, we confirmed that the activation of LXR signaling by T0901317 as well as the down-regulation of representative genes associated with specific biological pathways that could be linked to the therapeutic and pathologic effects of LXR activation. Our study demonstrated the potential of using zebrafish coupled with transcriptomic analysis for modeling toxicological or pathological effects and for screening of LXR modulators.

2. Experimental procedures

2.1. Zebrafish and T0901317 treatment

Adult male zebrafish (around 6 months old and 500–700 mg per fish) were obtained from a local fish supplier. To avoid complications that could be introduced due to reproductive cycle and hormonal changes as a result of the high fecundity and regular spawning in females, only male fish were used. The zebrafish were acclimatized for at least two weeks in aquaria before the experiments began and they were fed twice a day. Only healthy fish with normal swimming and feeding behaviors were selected for experiments with T0901317 (Sigma-Aldrich), which was dissolved in dimethyl sulfoxide (DMSO; Sigma-Aldrich) as a vehicle solvent. Final DMSO concentration in all treatments and control was 0.05% (v/v). Zebrafish were exposed to T0901317 at different concentrations (20 nM, 200 nM and 2000 nM) for 96 h with 10 fish in 2-L water per tank at 27 ± 2 °C. Chemical solutions and water were changed daily by transferring treated fish to new tanks. Fish were not fed throughout the experiment. All experiments were performed in accordance to the guidelines of Institutional Animal Care and Use Committee (IACUC) and approved by IACUC. Five independent sets of experiments were conducted, i.e. for histological analysis, hepatosomatic index, enzyme-colorimetric assays, microarray experiments and real-time PCR gene expression validation. The 96 h is chosen as a single end-point for all experiments because it is the end time-point for the standard 96-h acute zebrafish toxicity test which provides sufficient time for the cumulated effects of the agonist to occur and manifest in the liver including toxico-pathology. This would enable us to compare with endpoint data reported in mammalian models.

2.2. Hepatosomatic index

At the end of the experiment, wet weight of fish was first determined before dissecting the whole liver to be weighed. Hepatosomatic index was calculated based on the following formula: (wet weight of liver / wet weight of body) × 100. A total of $N = 7$ biological replicates were used.

2.3. Histological processing

At the end of the experiment, the peritoneal organs including the liver were fixed in Bouin's solution and in Formalin solution 10%, Neutral Buffered (Sigma-Aldrich) for 1 week at room temperature. The tissue samples were then washed several times with 70% ethanol, dehydrated in a series of increasing ethanol concentration (70%–100%), cleared in Histo-Clear and embedded in paraffin. The paraffin-embedded samples were sectioned sagittally at 5 μm thickness. The Bouin-fixed sections were stained with hematoxylin and eosin (H&E) for qualitative and quantitative assessment of liver parenchyma.

2.4. Histological examination

Histological assessment was performed with a compound microscope, Axioskop 2 (Zeiss®), for T0901317-induced phenotypic changes in liver parenchyma at tissue level. Hematoxylin and Eosin-stained liver sections from treated and control fish were compared for qualitative (i.e. visible changes in liver parenchyma) and quantitative (i.e. hepatocytes nuclei density) changes. Density of the hepatocyte nuclei (no. of hepatocyte nuclei/36,250 μm^3) was measured in T0901317-treated and control fish liver with the image analyzer program (Axiovision, Zeiss®). Anterior, middle and posterior regions of three liver sections were used to determine the density of hepatocytes nuclei from each replicate. Four biological replicates ($N = 4$) were assessed for each group. The statistical significance ($P < 0.01$, $P < 0.05$) of changes in density was determined using a heterocedastic Student's *t*-test.

2.5. Apoptotic staining

Apoptotic staining was performed on formalin-fixed paraffin-embedded sections using Apoptag®Plus Fluorescein In Situ Apoptosis Detection Kit according to manufacturer's protocol (Chemicon) to detect DNA fragmentations which are associated with cellular apoptosis in the liver.

2.6. Periodic acid-Schiff (PAS) staining

PAS is used to detect glycogen in tissue sections. Staining was performed on formalin-fixed paraffin-embedded sections using Alcian Blue PAS stain kit without diastase according to manufacturer's protocol (BioGenex).

2.7. Oil red O staining

Oil Red O is used to stain for lipids. Fresh frozen liver samples were sectioned with Cryostat Sectioning and stained with Oil Red O (Sigma-Aldrich). Sections were also counterstained with hematoxylin for contrast.

2.8. Triacylglycerol (triglyceride) and glycogen quantification

Triacylgycerol and glycogen levels in the liver were determined using the respective enzyme-colorimetric Triglyceride Quantification Kit (Biovision) and EnzyChrom™ Glycogen Assay Kit (Biovision) according to manufacturer's protocol. Triacylgycerol (nmol) and

glycogen (μg) levels were normalized to the protein level (μg) in the liver. The protein level in the liver was determined using a colorimetric Protein Quantitation Kit (Biovision) according to manufacturer's protocol. The statistical significance ($P<0.05$) of changes in relative gene expression level when compared to the control group was determined using a heterocedastic Student's *t*-test.

2.9. RNA extraction and DNA microarray experiments

For the microarray experiments, adult male zebrafish were exposed to T0901317 at 20 nM, 200 nM and 2000 nM with 0.05% (v/v) DMSO as vehicle for 96 h, whereas the control group was exposed to vehicle only. Five biological replicates were performed for each treatment group and each replicate consists of livers pooled from 4 individual male fish. Therefore, a total of 20 microarray hybridizations were performed on 20 pooled liver samples derived from 80 zebrafish for the three treatment groups and one control group.

Total RNAs from five replicates (each replicate consist of pooled livers from four fishes) after 96 hour treatment were isolated with Trizol reagent (Invitrogen, USA) protocol. Reference RNA was obtained by pooling total RNA from whole male and female wild-type zebrafish in 9:1 ratio. Reference RNA was co-hybridized with RNA samples either from control or treated fish on a poly-L-lysine-coated glass array spotted with 22 K zebrafish oligo probes. For fluorescence labeling of cDNAs, 10 μg of total RNA from the reference and sample RNAs were reverse transcribed and labeled differently, with fluorescent dyes Cy-3 and Cy-5, respectively. The microarray slides were hybridized at 42 °C for 16 h in hybridization chambers, then they were washed in a series of washing solutions (2× SSC with 0.1% SDS; 1× SSC with 0.1% SDS; 0.2× SSC and 0.05× SSC; 30 s each), dried with low-speed centrifugation and scanned for fluorescence detection with the GenePix 4000B scanner (Axon Instruments). Detailed protocols for microarray experiment and data acquisition using the zebrafish microarray can be referred [21,22].

2.10. Microarray data normalization and transcriptome analysis with gene set enrichment analysis (GSEA)

Lowess method in the R package (http://www.braju.com/R/) was used to normalize the raw microarray data. The microarray raw data have been formatted to be compliant with MIAME standard. The transcriptome data of each treatment group, i.e. Low (L, 20 nM), Mid (M, 200 nM), High (H, 2000 nM), and in one combined analysis group [Low, Mid and High (LMH)] were compared to the control group using *t*-test to generate a p-value for each gene in the respective group. The reason for combining the 3 treatment groups in the analysis is to increase statistical power for identifying gene with overall consistent expression trend (i.e. concentration-dependent perturbation) across the three concentrations. Gene set enrichment analysis (GSEA) [23] was performed to characterize the molecular pathways or processes that were perturbed by T0901317. The zebrafish genes were mapped to human homologs as previously described in [21]. The human homologs of zebrafish genes from the transcriptome profiles were ranked according to the p-values with Student *t*-test. The "GseaPreranked" option of GSEA was used. The ranking metric used was $\log_{10}$ (1/P) where P is the p-value of a gene from microarray data. Up-regulated genes are assigned positive values of $\log_{10}$ (1/P) whereas down-regulated genes are assigned negative values of $\log_{10}$ (1/P). The genes were later ranked in descending order based on values of $\log_{10}$ (1/P). The ranked list of genes for each concentration are compared to 1892 curated gene sets or molecular signatures that are deposited in the Molecular Signatures Database (MSigDB) from the GSEA website http://www.broadinstitute.org/gsea/index.jsp.

An enrichment score (ES) that reflects the degree to which a molecular signature (a pre-defined gene set) is over-represented at the top or bottom rank of the ranked whole transcriptome profile was calculated by 'walking' down the ranked profile. The ES is the maximum deviation from zero encountered in the random walk corresponds to a weighted Kolmogorov–Smirnov-like statistic. The ES for each molecular signature was normalized to the size of the set yielding a normalized enrichment score (NES). Statistical significance of a molecular signature for each concentration treatment was calculated using an empirical phenotype-based permutation test procedure. The number of permutation used was 1000. Molecular signature with false discovery rate (FDR) <0.25 was considered statistically significant, $0.25 \leq$ FDR <0.35 as marginally significant and FDR ≥ 0.35 were not significant. Positive and negative NES values indicate that if the over-represented genes were mostly correlated with the ranked up- or down-regulated genes, respectively.

2.11. Gene expression validation with real time quantitative PCR

Quantification of gene expression level was performed on synthesized First Strand cDNA via quantitative Real-Time PCR reaction using LightCycler® 480 SYBR Green I Master kit according to manufacturer's protocol (Roche). Nine biological replicates ($N=9$) in each concentration group were performed for all real-time PCR experiments. Quantification of transcript levels were measured by using relative quantification between PCR signal of the target transcript in treatment groups and untreated control group after normalization with the transcript level of 60S ribosomal protein L13a (*rpl13a*). Detailed information of primers used is provided in Additional file 1. The statistical significance ($P<0.1$, $P<0.05$) of changes in relative gene expression level when compared to the control group was determined using a heterocedastic Student's *t*-test.

3. Results and discussion

3.1. Histological analysis of T0901317-induced perturbations in zebrafish liver

Histological analysis was performed on the liver from male adult zebrafish exposed to a range of T0901317 concentrations to examine the histological changes caused by T0901317 toxicity. This will also help to establish the appropriate concentration that could induce perturbation leading to hepatotoxicity and hence the concentrations that will be used for subsequent microarray experiment. We observed concentration-dependent histological changes in the liver when fish were treated with 20 nM, 200 nM and 2000 nM of T0901317. We found that T0901317-treated liver parenchyma appeared to be less homogenous and the hepatocytes appeared to have swelled as they were larger and less regular in shape as T0901317 concentration increased when compared to the more compact, smaller and polygonal-shaped hepatocytes in the control group (Fig. 1A–D).Besides having larger size and irregular shape, the hepatocytes were observed to have clear cytoplasm and many without nucleus or with small fading nucleus in the liver of fish treated with 200 nM and 2000 nM of T0901317 (Fig. 1C and D) when compared to the pale pink granular cytoplasm with distinct nuclei in hepatocytes of fish treated with 20 nM of T0901317 or control group. Indeed, the number of hepatocyte nuclei per volume (36,250 μm^3) of the section stained with hematoxylin and eosin (H&E) was found to have reduced significantly as T0901317 concentration increased (Fig. 1E; see Experimental procedures). Since fish treated with 2000 nM T0901317 has the most significant reduction in hepatocyte nuclei per volume liver section, we further measured the hepatosomatic index and performed apoptotic staining (see Experimental procedures) to determine if liver enlargement and/or cell death may have caused the decrease in hepatocyte nuclei per volume liver section of fish treated with 2000 nM T0901317 compared to the control group. The mean hepatosomatic index of fish treated with 2000 nM T0901317 was found to have increased significantly (1.7-fold higher

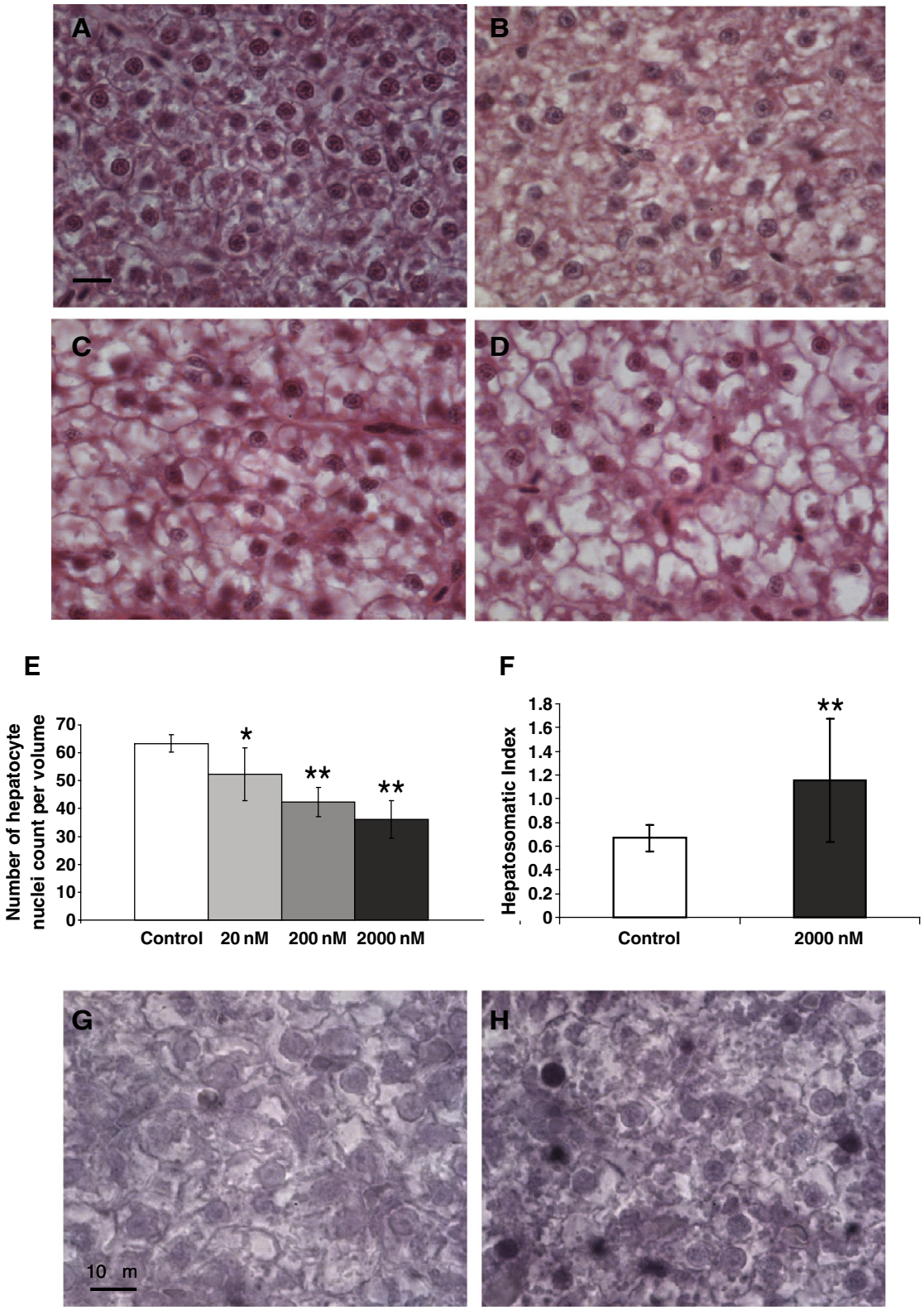

Fig. 1. Histological analysis of liver perturbation induced by T0901317. Hematoxylin and eosin (H&E) stained liver sections from adult male zebrafish exposed to (A) vehicle only (control, 0.05% DMSO), (B) 20 nM (C), 200 nM and (D) 2000 nM of T0901317. The livers from fish exposed to 200 nM and 2000 nM of T0901317 appeared less homogenous and the hepatocytes appeared larger and more irregular in shape compared to controls. (E) Concentration-dependent decrease in number of hepatocyte nuclei count per volume section (36,250 μm^3) in H&E stained liver sections from fish exposed to T0901317 compared to controls ($N = 4$ biological replicates; Student's t-test $^*P$-value < 0.1, $^{**}P$ value < 0.05). (F) Increase hepatosomatic index [(wet weight of liver / wet weight of body) $\times$ 100] of fish treated with 2000 nM T0901317 compared to control fish ($N = 7$ biological replicates; Student's t-test $^{**}P$-value < 0.05). Apoptotic staining in liver of control fish (G) compared to liver treat with 2000 nM T0901317 (H) showed increase apoptotic activity in treated liver. Scale bar represents 10 μm in panel (A) is applicable for panels (B–D), and in panel (G) is applicable to panel (H).

than control fish, $P<0.05$), suggesting that liver enlargement had occurred in fish treated with 2000 nM T0901317 (Fig. 1F). Interestingly, increased apoptotic staining was also observed in liver of fish treated with 2000 nM T0901317 compared to control group (Fig. 1G and H). Taken together, the findings suggest that the liver has enlarged and related hepatocyte ballooning which could also lead to cell death had occurred in the liver of fish treated with 2000 nM T0901317. Hepatocyte ballooning degeneration as indicated by cytoplasmic clearing and cell swelling with fading nuclei is known to be associated with liver histopathology [24]. Therefore, the decrease in hepatocyte nuclei per volume liver section could be due to liver swelling and related hepatocyte ballooning, and possibly cell death.

Since T0901317 and activation of LXR is known to regulate lipid and carbohydrate metabolisms, we performed oil-red O and PAS staining for lipid and glycogen accumulation, respectively, in liver of fish treated with T0901317. Oil-red O staining detected moderate increase of small vesicular lipid accumulation in some hepatocytes of fish treated with 200 nM (data not shown) and 2000 nM T0901317 (Fig. 2B) suggesting early or mild signs of hepatic steatosis when compared to 20 nM T0901317 (data not shown) and control fish (Fig. 2A). PAS staining revealed accumulation of glycogen, resembling glycogen storage disorder, in the liver of fish treated with 2000 nM T0901317 (Fig. 2D) when compared to control fish (Fig. 2C). Even so, the increase in lipid and glycogen accumulation in the liver was difficult to quantify using these special-stained liver sections. Since oil-red O and PAS staining for lipid and glycogen accumulation, respectively, were more apparent in the liver of fish treated with 2000 nM T0901317, we performed additional experiments to

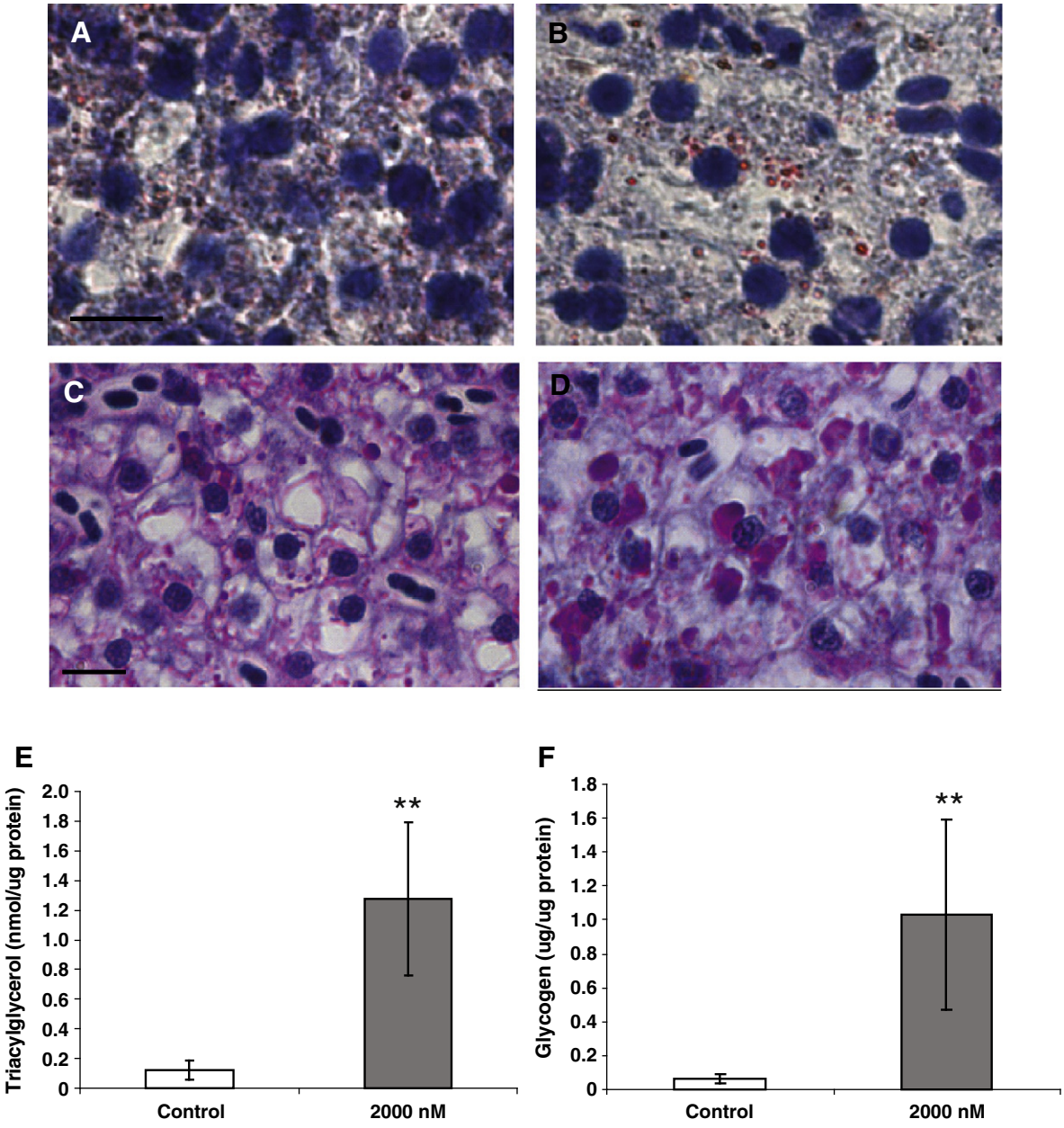

Fig. 2. Hepatic lipid and glycogen levels perturbed by T0901317. Oil Red O staining detected increased lipid vesicles (stained red) in liver of control fish (A) compared to liver of fish treated with 2000 nM of T0901317 (B). PAS staining detected increased glycogen accumulation (stained purple) in liver of control fish (C) compared to liver of fish treated with 2000 nM of T0901317 (D). Scale bar represents 10 μm in panels (A) and (C) are applicable to respective panels (B) and (D). Triacyglycerol level in liver of fish treated with 2000 nM T0901317 was significantly higher compared to control fish (E). Glycogen level in liver of fish treated with 2000 nM T0901317 was significantly higher compared to control fish (F). ($N=5$ biological replicates; Student's t-test $^{**}P$-value<0.05).

quantify the levels of triacylglycerol and glycogen using enzyme-colorimetric assays on liver of fish treated with 2000 nM T0901317 and control fish. We found that triacyglycerol levels in the liver of fish treated with 2000 nM T0901317 was 1.28 ± 0.52 nmol/μg protein (mean ± standard deviation) and has significantly ($P<0.001$) increased about 10-fold compared to the liver of control fish (0.12 ± 0.06 nmol/μg protein) (Fig. 2E). As for glycogen, it was found that the levels in the liver of fish treated with 2000 nM T0901317 was 1.03 ± 0.58 μg/μg protein and has significantly ($P<0.005$) increased about 16-fold compared to the liver of control fish (0.06 ± 0.03 μg/μg protein) (Fig. 2F). The findings further confirmed the lipid and glycogen accumulation in zebrafish liver as

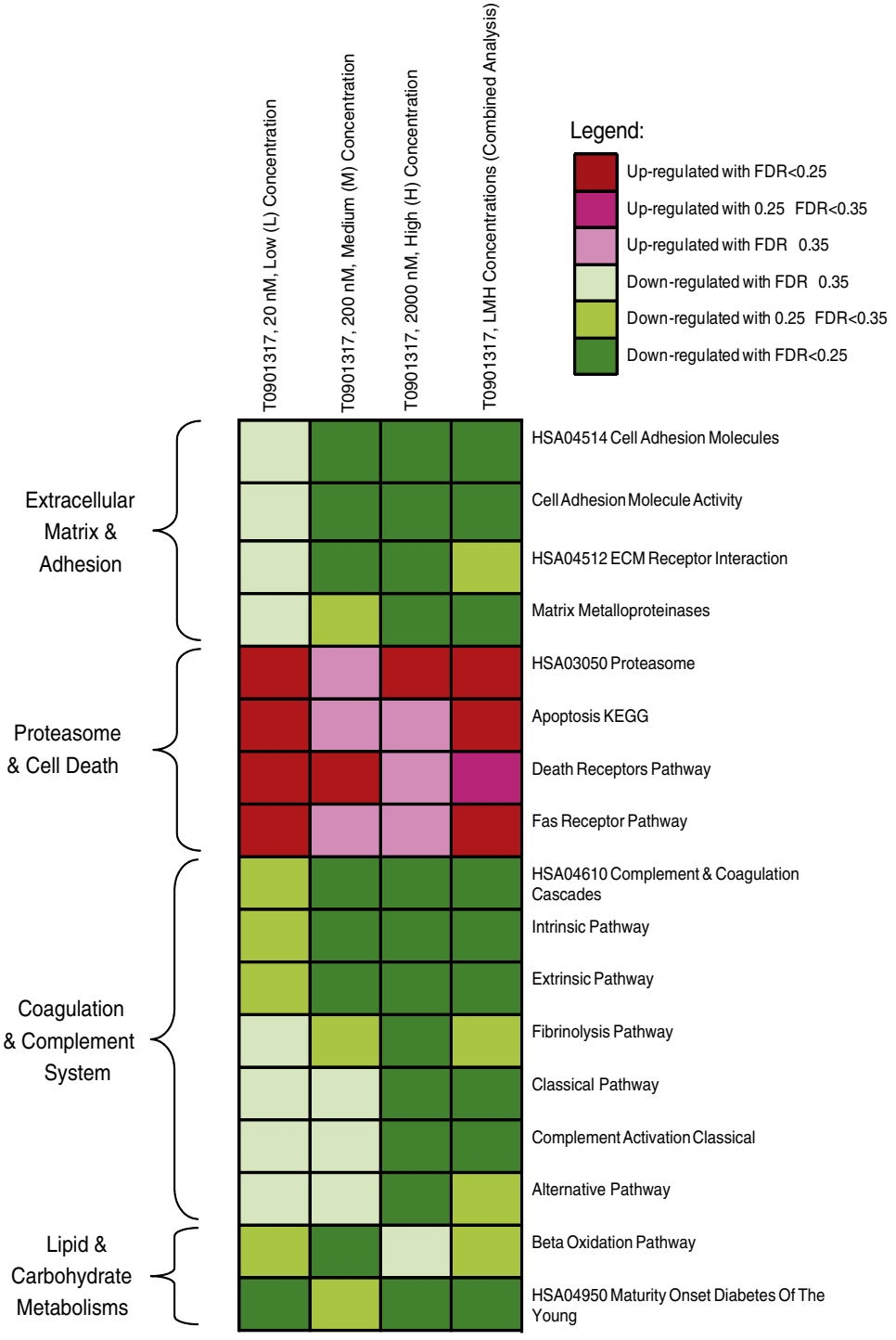

Fig. 3. Gene Set Enrichment Analysis (GSEA) of liver transcriptome of T0901317-treated zebrafish. GSEA analysis was carried out on the transcriptome profile of the treatment groups 20 nM, 200 nM, 2000 nM, and combined analysis group from Low, Mid and High (LMH) compared to control group. Seventeen molecular signatures that were up- or down-regulated with statistical significance (FDR <0.35) in at least two groupings were selected and shown as they demonstrated concentration-dependent profiles therefore gave greater confidence that the effects are correlated to T0901317-induced liver perturbation. The deregulated molecular signatures were further grouped into related processes: "Extracellular Matrix and Adhesion", "Proteasome and Cell Death", "Coagulation and Complement System" and "Lipid and Carbohydrate Metabolisms". Up- and down-regulated molecular signatures are indicated in different shades of red and green, respectively. The shades of red and green are based on significance value of false discovery rate (FDR) (see figure legend).

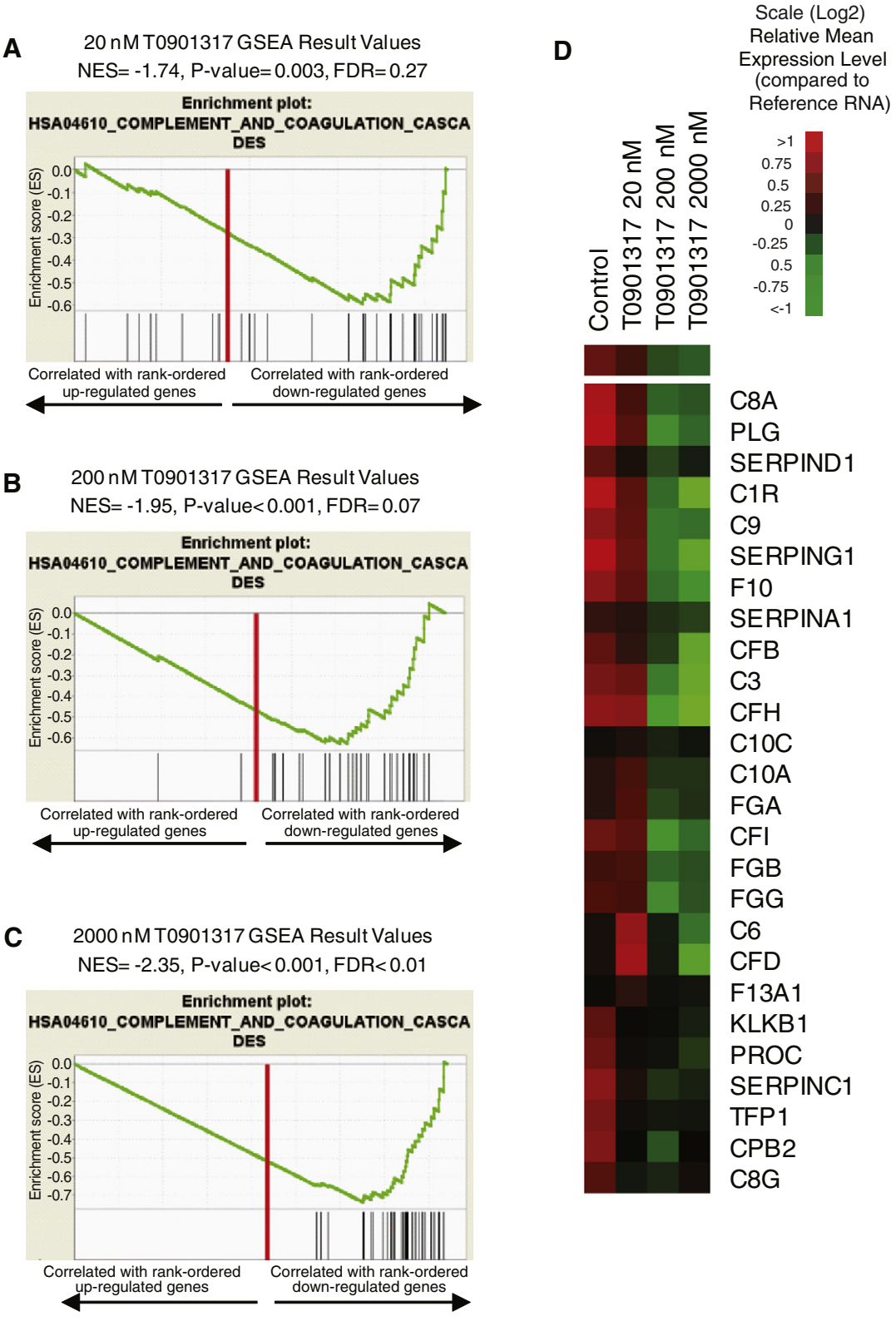

Fig. 4. Gene Set Enrichment Analysis revealed T0901317 induced concentration-dependent down-regulation of coagulation and complement cascades (HSA04610) as indicated by the decreasing Normalized Enrichment Score (NES), *P*-value and False Discovery Rate (FDR) value with increasing T0901317 concentration at (A) 20 nM, (B) 200 nM, and (C) 2000 nM. The enrichment plot (green) at the bottom panel indicates the enrichment score (y-axis) versus the rank-ordered non-redundant list of genes (x-axis) in the entire transcriptome profile. The vertical black lines represent the ranked position of genes associated with the coagulation and complement cascades molecular signature within the ranked list of genes in the entire transcriptome profile. Vertical black lines on the far left are correlated with rank-ordered up-regulated genes, while those on the far right are correlated with rank-ordered down-regulated genes. As T0901317 concentration increased, the vertical lines which represent genes in the coagulation and complement cascade are found in the far right correlating with rank-ordered down-regulated genes in the transcriptome profile. The vertical red bar indicates the position where there is zero correlation. (D) Hierarchical cluster analysis of 26 genes from coagulation and cascades (HSA04610) gene set demonstrate that their relative gene expression levels (above reference RNA) decreased with increasing T0901317 concentration.

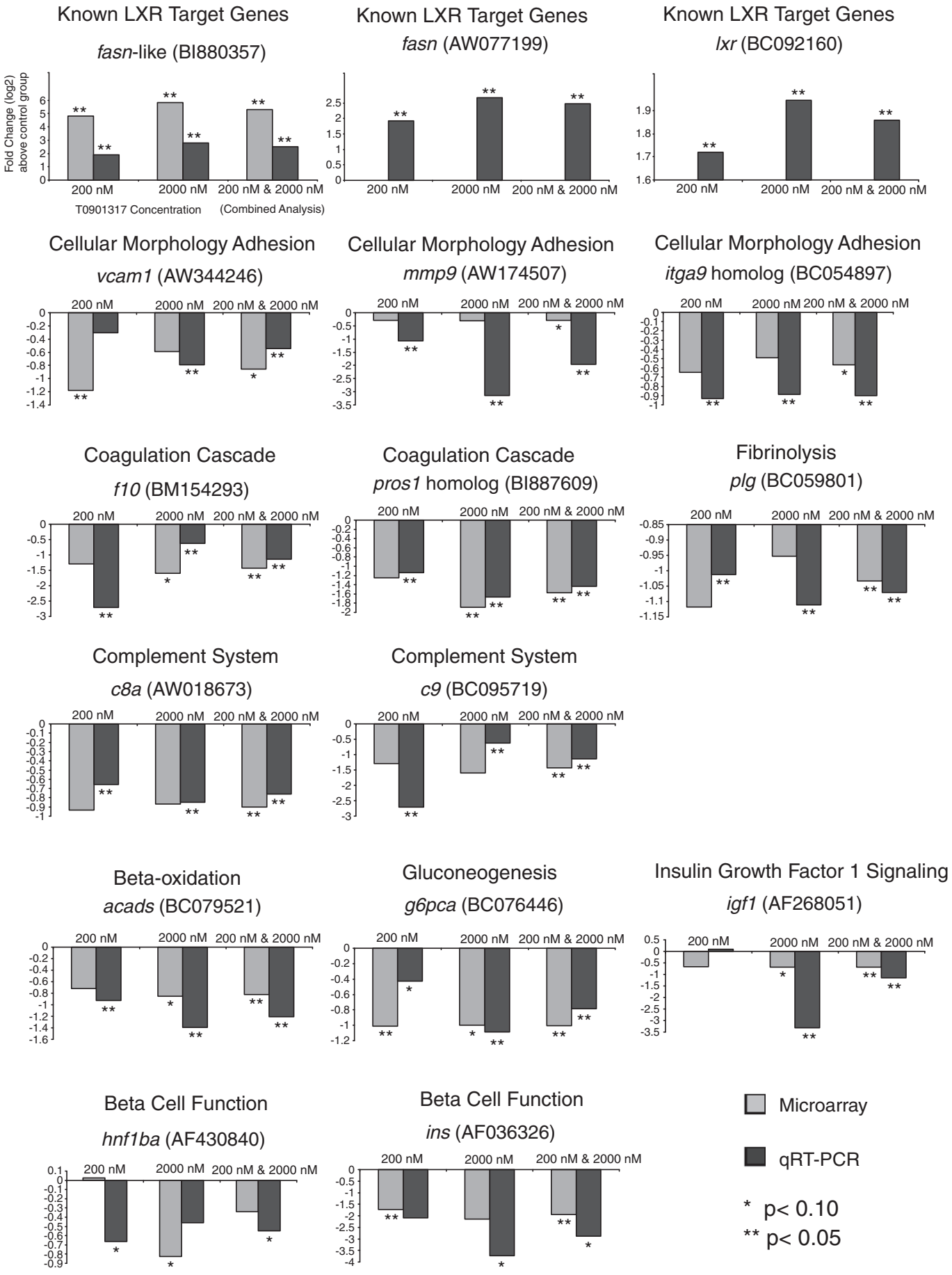
Known LXR Target Genes
fasn-like (BI880357)
Fold Change (log2) above control group
200 nM
2000 nM
200 nM & 2000 nM
T0901317 Concentration
(Combined Analysis)
Known LXR Target Genes
fasn (AW077199)
Known LXR Target Genes
lxr (BC092160)
Cellular Morphology Adhesion
vcam1 (AW344246)
Cellular Morphology Adhesion
mmp9 (AW174507)
Cellular Morphology Adhesion
itga9 homolog (BC054897)
Coagulation Cascade
f10 (BM154293)
Coagulation Cascade
pros1 homolog (BI887609)
Fibrinolysis
plg (BC059801)
Complement System
c8a (AW018673)
Complement System
c9 (BC095719)
Beta-oxidation
acads (BC079521)
Gluconeogenesis
g6pca (BC076446)
Insulin Growth Factor 1 Signaling
igf1 (AF268051)
Beta Cell Function
hnf1ba (AF430840)
Beta Cell Function
ins (AF036326)
Microarray
qRT-PCR
* p< 0.10
** p< 0.05

induced by T0901317. Lipid and glycogen accumulation in the liver are also known to cause hepatocyte swelling [24] which contributed to the observed liver histopathology and increased hepatosomatic index. Taken together with the histological evidence, the findings suggest that concentration-dependent perturbation leading to toxicity and injury could be induced in the liver of adult male zebrafish exposed to 20 nM, 200 nM and 2000 nM of T0901317. These concentrations were used for the subsequent microarray experiments.

3.2. Gene set enrichment analysis (GSEA) of T0901317-induced liver perturbation

GSEA was performed to characterize the molecular pathways or processes that were perturbed by T0901317. A Normalized Enrichment Score (NES) and a False Discovery Rate (FDR) value (corrected for multiple hypothesis testing) were generated for each of the molecular signature gene set to indicate the extent of the over-representation and its statistical significance, respectively. Based on the categories of FDR and NES values, profiles of the molecular signatures were analyzed across the four groupings (20 nM, 200 nM, 2000 nM or LMH combined analysis). In order to increase our likelihood of identifying molecular signatures that were perturbed by T0901317 in a concentration-dependent manner, we included in our analysis of molecular signatures that were consistently up- or down-regulated with marginal significance (FDR <0.35) in at least two groupings. Molecular signatures that demonstrate concentration-dependent profiles gave greater confidence that the effects are correlated to T0901317-induced liver perturbation. Using this criterion, we identified 17 molecular signatures from the GSEA output (Fig. 3). Most of the enriched molecular signatures are associated with cellular morphology and adhesion, cell death, coagulation cascade and complement system which demonstrated increasing or decreasing concentration-dependent perturbation by T0901317.

3.3. Coagulation and complement systems

Based on our transcriptomic analysis, T0901317 appeared to down-regulate molecular signatures associated with coagulation and complement system including Complement & Coagulation Cascades (HSA04610), Intrinsic Pathway, Extrinsic Pathway, Fibrinolysis Pathway, Classical Pathway and Complement Activation Classical Pathway (Fig. 3). These pathways displayed similar profiles as they involved overlapping genes. As shown in Fig. 4A–C, with increasing T0901317 concentration, both NES and FDR values decreased, indicating a statistical significance in increasing representation of genes in Complement & Coagulation Cascades. A closer examination of the 26 human homologs in the Complement & Coagulation Cascades signature revealed expression profiles that were generally in a down-regulated trend with increasing concentrations of T0901317 (Fig. 4D). Taken together, the analysis indicated that the molecular signature for Complement & Coagulation Cascades was down-regulated by T0901317-induced liver perturbation in an increasing concentration-dependent manner.

Interestingly, LXR activation has been shown to suppress the expression of tissue factor (TF), a major initiator of blood coagulation [25], in human islets [26] and mouse macrophages [27]. Macrophages are major source of TF contributing to thrombogenesis in atherosclerosis [27]. Hence, anti-thrombotic action via suppression of TF is one of the anti-atherosclerotic effects of LXR [8]. Our analysis revealed that various genes (*pros1, f10, tfpi, serpinc1* and *plg*) involved in the coagulation pathway, which could further be implicated with anti-thrombotic action, were also down-regulated by T0901317.

Moreover, activation of LXR by T0901317 was observed to down-regulate genes associated with the complement pathway, which is the part of innate immune system to activate inflammatory response. Chronic inflammation also contributes to atherogenesis [28] and there are lines of evidence that complement activation plays a major role in chronic inflammation that is associated with initiation and progression of atherosclerotic lesions [29] and also in rheumatoid arthritis [30]. Thus LXR-induced down-regulation of complement pathway, as shown in our data, may in turn suppress inflammatory responses, thus promoting anti-atherogenic effect [9] and ameliorating rheumatoid arthritis [11]. Taken together, our observations suggest that T0901317-induced perturbation has suppressive effects on the expression of coagulation and complement factors in the liver which in return could further contribute to its anti-thrombotic and anti-atherogenic actions.

3.4. Extracellular matrix and adhesion

We also observed that T0901317 causes down-regulation of molecular signatures associated with cellular morphology and adhesion, including Cell Adhesion Molecules (HSA04514), Cell Adhesion Molecule Activity, ECM Receptor Interaction (HSA04512) and Matrix Metalloproteinases (MMPs), in concentration dosage-dependent manner (Fig. 3). Modulations of these molecular signatures were likely associated with the histological changes in cell and tissue morphology as observed in the livers of T0901317-treated fish. LXR has been proposed as a potential therapeutic target for atherosclerotic therapy [13] and T0901317-induced LXR activation has been shown to suppress the expression of cellular adhesion molecules in atherogenic vascular tissues [31]. Moreover, it has been reported that inhibition of broad-spectrum of MMPs leads to reduction in atherogenic progression [32,33]. Here, we observed T0901317-induced down-regulation of molecular signature involving MMPs, supporting that suppression of MMPs expression by activated LXR (via T0901317) could be a mechanism to the anti-atherogenic action as reported in rodent studies [31].

3.5. Lipid and carbohydrate metabolisms

LXR is known to affect major carbohydrate and lipid metabolic pathways [6,7]. Therefore, the down-regulated molecular signatures also included Maturity Onset Diabetes of the Young (MODY) and Beta-oxidation Pathway (Fig. 3). MODY is an autosomal dominant monogenic form of type II diabetes characterized by insulin resistance and relative insulin deficiency. Down-regulation of genes associated with MODY suggests that T0901317-induced perturbation in beta cell function, hence promoting insulin deficiency and/or resistance, though it does not mean that the fish was experiencing MODY specifically. Down-regulation of Beta-oxidation pathway, where fatty acids are catabolized to generate energy, may be associated with the onset of hepatic lipogenesis as intracellular lipid accumulation was observed in liver of fish treated with T0901317 (Fig. 2B and E). Impaired beta-oxidation has been reported to promote hepatic steatosis [34].

3.6. Proteasome and cell death

Based on our transcriptomic analysis, molecular signatures associated with Proteasome (HSA03050), Apoptosis (KEGG), Death receptor and Fas receptor pathways was up-regulated by T0901317 (Fig. 3). Up-regulation of proteasome pathway suggests the need to increase protein degradation activity likely as a means of cellular detoxification due to intracellular accumulation of oxidized, damaged and misfolded

Fig. 5. Real-time PCR validation of selected representative genes of interest and comparison with microarray data. Using samples from an independent validation experiment ($N = 9$ biological replicates), genes representing biological pathways were validated by real-time PCR and compared with corresponding microarray data ($N = 5$ biological replicates). Statistical significance was determined using Student's *t*-test: *P*-value $< 0.1^{*}$, *P*-value $< 0.05^{**}$. Axis titles on the upper left histogram and figure legends on the lower right are applicable to all histograms. The 200 nM and 2000 nM are combined analysis group using combined experimental data from 200 nM and 2000 nM groups.

proteins. It has been demonstrated that the loss of proteasomes or inhibition of proteasome pathway can lead to the induction of apoptosis and liver injury [35]. When damaged or misfolded proteins build up, cells will up-regulate synthesis of proteasomes. However, if accumulation of such proteins exceeds the cell capacity to degrade them, apoptotic pathways will be activated and cell death occurs. Interestingly, molecular signatures associated with apoptosis were also significantly (FDR ≤ 0.25) up-regulated at even a low T0901317 concentration of 20 nM, which corroborates with our histological evidence suggesting hepatocyte ballooning degeneration (Fig. 1A–E). LXR activation by T0901317 has been reported to induce apoptosis in pancreatic beta cells [36], inhibited pancreatic beta cell viability and proliferation [37] and more recently has been shown to exert anti-proliferative effect via cytotoxicity and apoptosis in ovarian [38] and prostate [39] cancer cells. Our analysis suggests that T0901317-induced perturbation in the liver caused up-regulation in apoptosis signaling and is likely mediated by Death receptor and Fas receptor pathways. Acute and chronic liver toxicity including steatosis are known to be associated with the expression of Death and Fas receptors on the hepatocyte membrane rendering these cells more susceptible to apoptosis and subsequent liver injury [40,41].

3.7. Gene expression validation

The transcriptional down-regulation of the above-mentioned biological pathways is known to be associated with therapeutic and/or pathologic effects of LXR activation hence is of interest for validation. To further confirm T0901317-induced activation of LXR signaling and validate subsequent down-regulated biological pathways, we determined the relative expression level of selected representative genes by quantitative real-time RT-PCR using RNA from liver of a new batch of fish treated with 200 nM and 2000 nM T0901317 and control fish. The expression data from 200 nM and 2000 nM groups were also combined as a single group (200 nM and 2000 nM) for statistical analysis against the control group and both quantitative real-time RT-PCR and microarray data were compared.

The relative gene expression analysis of the quantitative real-time RT-PCR data showed good concordance with the microarray data in terms of expression direction and trend although the fold-change levels above respective control groups were different (Fig. 5). Statistical significance ($p<0.10$) were observed in almost all the groups in the real-time PCR data while statistical significance of microarray data were observed mainly in all the combined 200 nM and 2000 nM group albeit some genes were not significant when analyzed within respective 200 nM or 2000 nM group. The difference in the statistical significance is due to the more replicates ($N=9$ biological replicates) used in the real-time PCR data compared to the microarray data ($N=5$ biological replicates), hence providing greater statistical power to account for the noise level arising from the biological and technical variations.

Three known LXR-targeted genes, *lxr* itself, *fatty acid synthase (fasn)* (the probes for these two genes were not found in our microarray, hence there is no microarray data for them) and *fasn-like*, were up-regulated in a concentration-dependent manner confirming that T0901317 induced activation and up-regulation of LXR signaling pathway in the liver of treated fish which is consistent with mammalian data. Activated LXR is known to auto-regulate its own expression as demonstrated in various human cells [42] and also up-regulate *FASN* which modulates lipid metabolism [7]. We further inferred down-regulation of the following biological pathways in the liver of fish exposed to T0901317 by determining the relative expression levels of representative genes: *vascular cell adhesion molecule 1* (*vcam1*), *integrin, alpha 9* homolog (*ITGA9* homolog), *matrix metallopeptidase 9* (*mmp9*) for cellular morphology and adhesion; *coagulation factor X* (*f10*), *protein S alpha* homolog (*PROS1* homolog) for coagulation cascade; *plasminogen* (*plg*) for fibrinolysis; *complement component 8 alpha* (*c8a*), *complement component 9* (*c9*) for complement pathway; *acyl-coenzyme A dehydrogenase* short chain (*acads*) for beta-oxidation pathway, *glucose-6-phosphatase a, catalytic* (*g6pca*) for gluconeogenesis, *insulin-like growth factor 1*(*igf1*), *hepatocyte nuclear factor 1-beta-A* (*hnf1ba*), *insulin* (*ins*) for insulin signaling and related beta cell function. The expression level of these genes showed down-regulation trend in the liver of fish exposed to T0901317 and were all statistically significant ($p<0.10$) in the real-time PCR data (Fig. 5). Down-regulation of *g6pca*, which catalyzes the terminal step in the gluconeogenic and glycogenolytic, corroborates with the accumulation of glycogen observed in the histological analysis (Fig. 2D and F) and together with down-regulation of *acads* and up-regulation of *fasn* and *fasn-like*, are known to be associated with hepatic steatosis (Fig. 2B and E) [7,43]. Taken together, the up-regulation of LXR targeted genes, *lxr, fasn,* and *fasn-like*, suggests involvement of LXR activation and signaling in T0901317-induced liver perturbation which resulted in down-regulation in biological pathways such as extracellular matrix and adhesion, complement and coagulation systems, lipid and carbohydrate metabolisms.

Although LXR activation is known to suppress the gene expression and protein level of tissue factor (TF), an initiator of blood coagulation [26,27], and also suppress inflammatory responses [9], it is worth highlighting that suppression of gene expression associated with the coagulation and complement systems involving multiple genes (Fig. 4) by LXR activation has not been reported previously. Transcriptional repression by LXR on genes implicated in inflammation and lipid metabolism has been described [8,44–46]. It has been reported that nearly all of the LXR transrepression activities on genes involved with inflammatory signaling pathways in macrophages were shown to require interaction with nuclear receptor corepressor (NCor) and silencing mediator of retinoic acid and thyroid hormone receptor (SMRT) [45]. Our study suggests that zebrafish lxr may be involved in similar transcription repression of several biological pathways, and hence, it is plausible that complement and coagulation system could also be transrepressed by lxr via interaction with corepressors NCor and SMRT homologs which are known to be present in zebrafish.

4. Conclusions

In summary, in our efforts to use zebrafish for disease modeling, drug and toxicity screening, we have investigated T0901317-induced perturbation in the zebrafish liver and found several conserved effects of T0901317 with mammalian models including up-regulation of LXR-targeted genes, modulation of biological pathways associated with cell death, extracellular matrix and adhesions, carbohydrate and lipid metabolisms. In addition to the known pathways, the study also identified that the complement and coagulation systems were down-regulated by T0901317 induced LXR activation. These biological pathways down-regulated by T0901317 could be linked to the anti-thrombogenic, anti-atherogenic and anti-inflammatory actions, as well as metabolic disruptions via LXR activation. Our study highlights the potential of using zebrafish liver coupled with transcriptomic analysis to capture pharmacological and toxicological or pathological events induced by LXR modulators. The molecular signatures and validated genes identified in this study can serve as a reference for drug and toxicity screening of LXR modulators using the zebrafish model.

Supplementary materials related to this article can be found online at doi:10.1016/j.bbagen.2011.10.009.

Acknowledgments

This work is supported by Environment and Water Industry (EWI) Development Council of Singapore and BioMedical Research Council (BMRC) of Singapore.

References

[1] J.L. Collins, A.M. Fivush, M.A. Watson, C.M. Galardi, M.C. Lewis, L.B. Moore, D.J. Parks, J.G. Wilson, T.K. Tippin, J.G. Binz, K.D. Plunket, D.G. Morgan, E.J. Beaudet, K.D. Whitney, S.A. Kliewer, T.M. Willson, Identification of a nonsteroidal liver X receptor agonist through parallel array synthesis of tertiary amines, J. Med. Chem. 45 (2002) 1963–1966.

[2] D.W. Russell, Nuclear orphan receptors control cholesterol catabolism, Cell 97 (1999) 539–542.

[3] J.J. Repa, S.D. Turley, J.A. Lobaccaro, J. Medina, L. Li, K. Lustig, B. Shan, R.A. Heyman, J.M. Dietschy, D.J. Mangelsdorf, Regulation of absorption and ABC1-mediated efflux of cholesterol by RXR heterodimers, Science 289 (2000) 1524–1529.

[4] A. Archer, G. Lauter, G. Hauptmann, A. Mode, J.A. Gustafsson, Transcriptional activity and developmental expression of liver X receptor (lxr) in zebrafish, Dev. Dyn. 237 (2008) 1090–1098.

[5] J.M. Maglich, J.A. Caravella, M.H. Lambert, T.M. Willson, J.T. Moore, L. Ramamurthy, The first completed genome sequence from a teleost fish (Fugu rubripes) adds significant diversity to the nuclear receptor superfamily, Nucleic Acids Res. 31 (2003) 4051–4058.

[6] B.A. Laffitte, L.C. Chao, J. Li, R. Walczak, S. Hummasti, S.B. Joseph, A. Castrillo, D.C. Wilpitz, D.J. Mangelsdorf, J.L. Collins, E. Saez, P. Tontonoz, Activation of liver X receptor improves glucose tolerance through coordinate regulation of glucose metabolism in liver and adipose tissue, Proc. Natl. Acad. Sci. U. S. A. 100 (2003) 5419–5424.

[7] M. Baranowski, Biological role of liver X receptors, J. Physiol. Pharmacol. 59 (Suppl 7) (2008) 31–55.

[8] S.B. Joseph, E. McKilligin, L. Pei, M.A. Watson, A.R. Collins, B.A. Laffitte, M. Chen, G. Noh, J. Goodman, G.N. Hagger, J. Tran, T.K. Tippin, X. Wang, A.J. Lusis, W.A. Hsueh, R.E. Law, J.L. Collins, T.M. Willson, P. Tontonoz, Synthetic LXR ligand inhibits the development of atherosclerosis in mice, Proc. Natl. Acad. Sci. U. S. A. 99 (2002) 7604–7609.

[9] N. Zelcer, P. Tontonoz, Liver X receptors as integrators of metabolic and inflammatory signaling, J. Clin. Invest. 116 (2006) 607–614.

[10] G. Cao, Y. Liang, C.L. Broderick, B.A. Oldham, T.P. Beyer, R.J. Schmidt, Y. Zhang, K.R. Stayrook, C. Suen, K.A. Otto, A.R. Miller, J. Dai, P. Foxworthy, H. Gao, T.P. Ryan, X.C. Jiang, T.P. Burris, P.I. Eacho, G.J. Etgen, Antidiabetic action of a liver x receptor agonist mediated by inhibition of hepatic gluconeogenesis, J. Biol. Chem. 278 (2003) 1131–1136.

[11] S.R. Chintalacharuvu, G.E. Sandusky, T.P. Burris, G.C. Burmer, S. Nagpal, Liver X receptor is a therapeutic target in collagen-induced arthritis, Arthritis Rheum. 56 (2007) 1365–1367.

[12] X. Li, V. Yeh, V. Molteni, Liver X receptor modulators: a review of recently patented compounds (2007–2009), Expert Opin. Ther. Pat. 20 (2010) 535–562.

[13] J.J. Repa, D.J. Mangelsdorf, The liver X receptor gene team: potential new players in atherosclerosis, Nat. Med. 8 (2002) 1243–1248.

[14] J.W. Chisholm, J. Hong, S.A. Mills, R.M. Lawn, The LXR ligand T0901317 induces severe lipogenesis in the db/db diabetic mouse, J. Lipid Res. 44 (2003) 2039–2048.

[15] A. Schlegel, D.Y. Stainier, Lessons from “lower” organisms: what worms, flies, and zebrafish can teach us about human energy metabolism, PLoS Genet. 3 (2007) e199.

[16] C. Sullivan, C.H. Kim, Zebrafish as a model for infectious disease and immune function, Fish Shellfish Immunol. 25 (2008) 341–350.

[17] P. Jagadeeswaran, Zebrafish: a tool to study hemostasis and thrombosis, Curr. Opin. Hematol. 12 (2005) 149–152.

[18] H.M. Stern, L.I. Zon, Cancer genetics and drug discovery in the zebrafish, Nat. Rev. Cancer 3 (2003) 533–539.

[19] H. Sukardi, H.T. Chng, E.C. Chan, Z. Gong, S.H. Lam, Zebrafish for drug toxicity screening: bridging the in vitro cell-based models and in vivo mammalian models, Expert Opin. Drug Metab. Toxicol. 7 (2011) 579–589.

[20] S.H. Lam, S. Mathavan, Y. Tong, H. Li, R.K. Karuturi, Y. Wu, V.B. Vega, E.T. Liu, Z. Gong, Zebrafish whole-adult-organism chemogenomics for large-scale predictive and discovery chemical biology, PLoS Genet. 4 (2008) e1000121.

[21] S.H. Lam, R. Krishna Murthy Karuturi, Z. Gong, Zebrafish spotted-microarray for genome-wide expression profiling experiments: data acquisition and analysis, Methods Mol. Biol. 546 (2009) 197–226.

[22] S.H. Lam, S. Mathavan, Z. Gong, Zebrafish spotted-microarray for genome-wide expression profiling experiments. Part I: array printing and hybridization, Methods Mol. Biol. 546 (2009) 175–195.

[23] A. Subramanian, P. Tamayo, V.K. Mootha, S. Mukherjee, B.L. Ebert, M.A. Gillette, A. Paulovich, S.L. Pomeroy, T.R. Golub, E.S. Lander, J.P. Mesirov, Gene set enrichment analysis: a knowledge-based approach for interpreting genome-wide expression profiles, Proc. Natl. Acad. Sci. U. S. A. 102 (2005) 15545–15550.

[24] Z.D. Goodman, H.R. Makhlouf (Eds.), Hepatic Histopathology, Lippincott Williams & Wilkins, 2007, 245–311 pp.

[25] E. Camerer, A.B. Kolsto, H. Prydz, Cell biology of tissue factor, the principal initiator of blood coagulation, Thromb. Res. 81 (1996) 1–41.

[26] H. Scholz, T. Lund, M.K. Dahle, J.L. Collins, O. Korsgren, J.E. Wang, A. Foss, The synthetic liver X receptor agonist GW3965 reduces tissue factor production and inflammatory responses in human islets in vitro, Diabetologia 52 (2009) 1352–1362.

[27] N. Terasaka, A. Hiroshima, A. Ariga, S. Honzumi, T. Koieyama, T. Inaba, T. Fujiwara, Liver X receptor agonists inhibit tissue factor expression in macrophages, FEBS J. 272 (2005) 1546–1556.

[28] A.J. Lusis, Atherosclerosis, Nature 407 (2000) 233–241.

[29] F. Niculescu, H. Rus, Complement activation and atherosclerosis, Mol. Immunol. 36 (1999) 949–955.

[30] M. Okroj, D. Heinegard, R. Holmdahl, A.M. Blom, Rheumatoid arthritis and the complement system, Ann. Med. 39 (2007) 517–530.

[31] L. Verschuren, J. de Vries-van, S. der Weij, R. Zadelaar, T. Kooistra Kleemann, LXR agonist suppresses atherosclerotic lesion growth and promotes lesion regression in apoE*3Leiden mice: time course and mechanisms, J. Lipid. Res. 50 (2009) 301–311.

[32] A.H. Baker, D.R. Edwards, G. Murphy, Metalloproteinase inhibitors: biological actions and therapeutic opportunities, J. Cell Sci. 115 (2002) 3719–3727.

[33] M.F. Prescott, W.K. Sawyer, J. Von Linden-Reed, M. Jeune, M. Chou, S.L. Caplan, A.Y. Jeng, Effect of matrix metalloproteinase inhibition on progression of atherosclerosis and aneurysm in LDL receptor-deficient mice overexpressing MMP-3, MMP-12, and MMP-13 and on restenosis in rats after balloon injury, Ann. N. Y. Acad. Sci. 878 (1999) 179–190.

[34] Y. Wei, R.S. Rector, J.P. Thyfault, J.A. Ibdah, Nonalcoholic fatty liver disease and mitochondrial dysfunction, World J. Gastroenterol. 14 (2008) 193–199.

[35] S.W. French, F. Bardag-Gorce, Ubiquitin-Proteasome Pathway in the Pathogenesis of Liver Disease, Springer Verlag, Berlin, 2005.

[36] S.S. Choe, A.H. Choi, J.W. Lee, K.H. Kim, J.J. Chung, J. Park, K.M. Lee, K.G. Park, I.K. Lee, J.B. Kim, Chronic activation of liver X receptor induces beta-cell apoptosis through hyperactivation of lipogenesis: liver X receptor-mediated lipotoxicity in pancreatic beta-cells, Diabetes 56 (2007) 1534–1543.

[37] Z.X. Meng, J. Nie, J.J. Ling, J.X. Sun, Y.X. Zhu, L. Gao, J.H. Lv, D.Y. Zhu, Y.J. Sun, X. Han, Activation of liver X receptors inhibits pancreatic islet beta cell proliferation through cell cycle arrest, Diabetologia 52 (2009) 125–135.

[38] J.J. Rough, M.A. Monroy, S. Yerrum, J.M. Daly, Anti-proliferative effect of LXR agonist T0901317 in ovarian carcinoma cells, J. Ovarian Res. 3 (2010) 13.

[39] A.J. Pommier, G. Alves, E. Viennois, S. Bernard, Y. Communal, B. Sion, G. Marceau, C. Damon, K. Mouzat, F. Caira, S. Baron, J.M. Lobaccaro, Liver X Receptor activation downregulates AKT survival signaling in lipid rafts and induces apoptosis of prostate cancer cells, Oncogene 29 (2010) 2712–2723.

[40] A.E. Feldstein, A. Canbay, P. Angulo, M. Taniai, L.J. Burgart, K.D. Lindor, G.J. Gores, Hepatocyte apoptosis and fas expression are prominent features of human nonalcoholic steatohepatitis, Gastroenterology 125 (2003) 437–443.

[41] P.S. Ribeiro, H. Cortez-Pinto, S. Sola, R.E. Castro, R.M. Ramalho, A. Baptista, M.C. Moura, M.E. Camilo, C.M. Rodrigues, Hepatocyte apoptosis, expression of death receptors, and activation of NF-kappaB in the liver of nonalcoholic and alcoholic steatohepatitis patients, Am. J. Gastroenterol. 99 (2004) 1708–1717.

[42] B.A. Laffitte, S.B. Joseph, R. Walczak, L. Pei, D.C. Wilpitz, J.L. Collins, P. Tontonoz, Autoregulation of the human liver X receptor alpha promoter, Mol. Cell. Biol. 21 (2001) 7558–7568.

[43] J.C. Hutton, R.M. O'Brien, Glucose-6-phosphatase catalytic subunit gene family, J. Biol. Chem. 284 (2009) 29241–29245.

[44] F. Blaschke, Y. Takata, E. Caglayan, A. Collins, P. Tontonoz, W.A. Hsueh, R.K. Tangirala, A nuclear receptor corepressor-dependent pathway mediates suppression of cytokine-induced C-reactive protein gene expression by liver X receptor, Circ. Res. 99 (2006) e88–e99.

[45] S. Ghisletti, W. Huang, K. Jepsen, C. Benner, G. Hardiman, M.G. Rosenfeld, C.K. Glass, Cooperative NCoR/SMRT interactions establish a corepressor-based strategy for integration of inflammatory and anti-inflammatory signaling pathways, Genes Dev. 23 (2009) 681–693.

[46] H. Wang, Y. Zhang, E. Yehuda-Shnaidman, A.V. Medvedev, N. Kumar, K.W. Daniel, J. Robidoux, M.P. Czech, D.J. Mangelsdorf, S. Collins, Liver X receptor alpha is a transcriptional repressor of the uncoupling protein 1 gene and the brown fat phenotype, Mol. Cell. Biol. 28 (2008) 2187–2200.